UC Berkeley
UC Berkeley Previously Published Works

Title
Measurement of Ds+ and Ds*+ production in B meson decays and from continuum e+e- annihilation at √s = 10.6 GeV

Permalink
https://escholarship.org/uc/item/97g0m6ss

Journal
Physical Review D - Particles, Fields, Gravitation and Cosmology, 65(9)

ISSN
0556-2821

Authors
Aubert, B
Boutigny, D
Gaillard, JM
et al.

Measurement of D_s^+ and D_s^{*+} production in B meson decays and from continuum e^+e^- annihilation at $\sqrt{s}=10.6$ GeV

B. Aubert,[1] D. Boutigny,[1] J.-M. Gaillard,[1] A. Hicheur,[1] Y. Karyotakis,[1] J. P. Lees,[1] P. Robbe,[1] V. Tisserand,[1] A. Palano,[2] A. Pompili,[2] G. P. Chen,[3] J. C. Chen,[3] N. D. Qi,[3] G. Rong,[3] P. Wang,[3] Y. S. Zhu,[3] G. Eigen,[4] B. Stugu,[4] G. S. Abrams,[5] A. W. Borgland,[5] A. B. Breon,[5] D. N. Brown,[5] J. Button-Shafer,[5] R. N. Cahn,[5] A. R. Clark,[5] M. S. Gill,[5] A. V. Gritsan,[5] Y. Groysman,[5] R. G. Jacobsen,[5] R. W. Kadel,[5] J. Kadyk,[5] L. T. Kerth,[5] Yu. G. Kolomensky,[5] J. F. Kral,[5] C. LeClerc,[5] M. E. Levi,[5] G. Lynch,[5] P. J. Oddone,[5] A. Perazzo,[5] M. Pripstein,[5] N. A. Roe,[5] A. Romosan,[5] M. T. Ronan,[5] V. G. Shelkov,[5] A. V. Telnov,[5] W. A. Wenzel,[5] P. G. Bright-Thomas,[6] T. J. Harrison,[6] C. M. Hawkes,[6] D. J. Knowles,[6] S. W. O'Neale,[6] R. C. Penny,[6] A. T. Watson,[6] N. K. Watson,[6] T. Deppermann,[7] K. Goetzen,[7] H. Koch,[7] M. Kunze,[7] B. Lewandowski,[7] K. Peters,[7] H. Schmuecker,[7] M. Steinke,[7] J. C. Andress,[8] N. R. Barlow,[8] W. Bhimji,[8] N. Chevalier,[8] P. J. Clark,[8] W. N. Cottingham,[8] N. Dyce,[8] B. Foster,[8] C. Mackay,[8] D. Wallom,[8] F. F. Wilson,[8] K. Abe,[9] C. Hearty,[9] T. S. Mattison,[9] J. A. McKenna,[9] D. Thiessen,[9] S. Jolly,[10] A. K. McKemey,[10] V. E. Blinov,[11] A. D. Bukin,[11] D. A. Bukin,[11] A. R. Buzykaev,[11] V. B. Golubev,[11] V. N. Ivanchenko,[11] A. A. Korol,[11] E. A. Kravchenko,[11] A. P. Onuchin,[11] A. A. Salnikov,[11] S. I. Serednyakov,[11] Yu. I. Skovpen,[11] V. I. Telnov,[11] A. N. Yushkov,[11] D. Best,[12] M. Chao,[12] A. J. Lankford,[12] M. Mandelkern,[12] S. McMahon,[12] D. P. Stoker,[12] K. Arisaka,[13] C. Buchanan,[13] S. Chun,[13] D. B. MacFarlane,[14] S. Prell,[14] Sh. Rahatlou,[14] G. Raven,[14] V. Sharma,[14] C. Campagnari,[15] B. Dahmes,[15] P. A. Hart,[15] N. Kuznetsova,[15] S. L. Levy,[15] O. Long,[15] A. Lu,[15] J. D. Richman,[15] W. Verkerke,[15] M. Witherell,[15] S. Yellin,[15] J. Beringer,[16] D. E. Dorfan,[16] A. M. Eisner,[16] A. A. Grillo,[16] M. Grothe,[16] C. A. Heusch,[16] R. P. Johnson,[16] W. S. Lockman,[16] T. Pulliam,[16] H. Sadrozinski,[16] T. Schalk,[16] R. E. Schmitz,[16] B. A. Schumm,[16] A. Seiden,[16] M. Turri,[16] W. Walkowiak,[16] D. C. Williams,[16] M. G. Wilson,[16] E. Chen,[17] G. P. Dubois-Felsmann,[17] A. Dvoretskii,[17] D. G. Hitlin,[17] S. Metzler,[17] J. Oyang,[17] F. C. Porter,[17] A. Ryd,[17] A. Samuel,[17] M. Weaver,[17] S. Yang,[17] R. Y. Zhu,[17] S. Devmal,[18] T. L. Geld,[18] S. Jayatilleke,[18] G. Mancinelli,[18] B. T. Meadows,[18] M. D. Sokoloff,[18] T. Barillari,[19] P. Bloom,[19] M. O. Dima,[19] S. Fahey,[19] W. T. Ford,[19] D. R. Johnson,[19] U. Nauenberg,[19] A. Olivas,[19] P. Rankin,[19] J. Roy,[19] S. Sen,[19] J. G. Smith,[19] W. C. van Hoek,[19] D. L. Wagner,[19] J. Blouw,[20] J. L. Harton,[20] M. Krishnamurthy,[20] A. Soffer,[20] W. H. Toki,[20] R. J. Wilson,[20] J. Zhang,[20] R. Aleksan,[21] A. de Lesquen,[21] S. Emery,[21] A. Gaidot,[21] S. F. Ganzhur,[21] P.-F. Giraud,[21] G. Hamel de Monchenault,[21] W. Kozanecki,[21] M. Langer,[21] G. W. London,[21] B. Mayer,[21] B. Serfass,[21] G. Vasseur,[21] Ch. Yèche,[21] M. Zito,[21] T. Brandt,[22] J. Brose,[22] T. Colberg,[22] M. Dickopp,[22] R. S. Dubitzky,[22] A. Hauke,[22] E. Maly,[22] R. Müller-Pfefferkorn,[22] S. Otto,[22] K. R. Schubert,[22] R. Schwierz,[22] B. Spaan,[22] L. Wilden,[22] D. Bernard,[23] G. R. Bonneaud,[23] F. Brochard,[23] J. Cohen-Tanugi,[23] S. Ferrag,[23] E. Roussot,[23] S. T'Jampens,[23] Ch. Thiebaux,[23] G. Vasileiadis,[23] M. Verderi,[23] A. Anjomshoaa,[24] R. Bernet,[24] A. Khan,[24] D. Lavin,[24] F. Muheim,[24] S. Playfer,[24] J. E. Swain,[24] J. Tinslay,[24] M. Falbo,[25] C. Borean,[26] C. Bozzi,[26] S. Dittongo,[26] L. Piemontese,[26] E. Treadwell,[27] F. Anulli,[28,*] R. Baldini-Ferroli,[28] A. Calcaterra,[28] R. de Sangro,[28] D. Falciai,[28] G. Finocchiaro,[28] P. Patteri,[28] I. M. Peruzzi,[28,*] M. Piccolo,[28] Y. Xie,[28] A. Zallo,[28] S. Bagnasco,[29] A. Buzzo,[29] R. Contri,[29] G. Crosetti,[29] M. Lo Vetere,[29] M. Macri,[29] M. R. Monge,[29] S. Passaggio,[29] F. C. Pastore,[29] C. Patrignani,[29] M. G. Pia,[29] E. Robutti,[29] A. Santroni,[29] S. Tosi,[29] M. Morii,[30] R. Bartoldus,[31] R. Hamilton,[31] U. Mallik,[31] J. Cochran,[32] H. B. Crawley,[32] P.-A. Fischer,[32] J. Lamsa,[32] W. T. Meyer,[32] E. I. Rosenberg,[32] G. Grosdidier,[33] C. Hast,[33] A. Höcker,[33] H. M. Lacker,[33] S. Laplace,[33] V. Lepeltier,[33] A. M. Lutz,[33] S. Plaszczynski,[33] M. H. Schune,[33] S. Trincaz-Duvoid,[33] G. Wormser,[33] R. M. Bionta,[34] V. Brigljević,[34] D. J. Lange,[34] M. Mugge,[34] K. van Bibber,[34] D. M. Wright,[34] M. Carroll,[35] J. R. Fry,[35] E. Gabathuler,[35] R. Gamet,[35] M. George,[35] M. Kay,[35] D. J. Payne,[35] R. J. Sloane,[35] C. Touramanis,[35] M. L. Aspinwall,[36] D. A. Bowerman,[36] P. D. Dauncey,[36] U. Egede,[36] I. Eschrich,[36] N. J. W. Gunawardane,[36] J. A. Nash,[36] P. Sanders,[36] D. Smith,[36] D. E. Azzopardi,[37] J. J. Back,[37] P. Dixon,[37] P. F. Harrison,[37] R. J. L. Potter,[37] H. W. Shorthouse,[37] P. Strother,[37] P. B. Vidal,[37] M. I. Williams,[37] G. Cowan,[38] S. George,[38] M. G. Green,[38] A. Kurup,[38] C. E. Marker,[38] P. McGrath,[38] T. R. McMahon,[38] S. Ricciardi,[38] F. Salvatore,[38] I. Scott,[38] G. Vaitsas,[38] D. Brown,[39] C. L. Davis,[39] J. Allison,[40] R. J. Barlow,[40] J. T. Boyd,[40] A. C. Forti,[40] J. Fullwood,[40] F. Jackson,[40] G. D. Lafferty,[40] N. Savvas,[40] E. T. Simopoulos,[40] J. H. Weatherall,[40] A. Farbin,[41] A. Jawahery,[41] V. Lillard,[41] J. Olsen,[41] D. A. Roberts,[41] J. R. Schieck,[41] G. Blaylock,[42] C. Dallapiccola,[42] K. T. Flood,[42] S. S. Hertzbach,[42] R. Kofler,[42] V. G. Koptchev,[42] T. B. Moore,[42] H. Staengle,[42] S. Willocq,[42] B. Brau,[43] R. Cowan,[43] G. Sciolla,[43] F. Taylor,[43] R. K. Yamamoto,[43] M. Milek,[44] P. M. Patel,[44] F. Palombo,[45] J. M. Bauer,[46] L. Cremaldi,[46] V. Eschenburg,[46] R. Kroeger,[46] J. Reidy,[46] D. A. Sanders,[46] D. J. Summers,[46] J. P. Martin,[47] J. Y. Nief,[47] R. Seitz,[47] P. Taras,[47] V. Zacek,[47] H. Nicholson,[48] C. S. Sutton,[48] C. Cartaro,[49] N. Cavallo,[49,†] G. De Nardo,[49] F. Fabozzi,[49] C. Gatto,[49] L. Lista,[49] P. Paolucci,[49] D. Piccolo,[49] C. Sciacca,[49] J. M. LoSecco,[50] J. R. G. Alsmiller,[51] T. A. Gabriel,[51] T. Handler,[51] J. Brau,[52] R. Frey,[52] M. Iwasaki,[52] N. B. Sinev,[52] D. Strom,[52] F. Colecchia,[53] F. Dal Corso,[53] A. Dorigo,[53] F. Galeazzi,[53] M. Margoni,[53] G. Michelon,[53] M. Morandin,[53] M. Posocco,[53] M. Rotondo,[53] F. Simonetto,[53] R. Stroili,[53] E. Torassa,[53] C. Voci,[53] M. Benayoun,[54] H. Briand,[54] J. Chauveau,[54] P. David,[54] Ch. de la Vaissière,[54] L. Del Buono,[54] O. Hamon,[54] F. Le Diberder,[54] Ph. Leruste,[54] J. Ocariz,[54] L. Roos,[54] J. Stark,[54] S. Versillé,[54] P. F. Manfredi,[55] V. Re,[55] V. Speziali,[55] E. D. Frank,[56] L. Gladney,[56] Q. H. Guo,[56] J. Panetta,[56] C. Angelini,[57] G. Batignani,[57] S. Bettarini,[57] M. Bondioli,[57] M. Carpinelli,[57] F. Forti,[57] M. A. Giorgi,[57] A. Lusiani,[57] F. Martinez-Vidal,[57] M. Morganti,[57] N. Neri,[57] E. Paoloni,[57] M. Rama,[57] G. Rizzo,[57] F. Sandrelli,[57] G. Simi,[57] G. Triggiani,[57] J. Walsh,[57] M. Haire,[58] D. Judd,[58] K. Paick,[58]

L. Turnbull,[58] D. E. Wagoner,[58] J. Albert,[59] P. Elmer,[59] C. Lu,[59] K. T. McDonald,[59] V. Miftakov,[59] S. F. Schaffner,[59]
A. J. S. Smith,[59] A. Tumanov,[59] E. W. Varnes,[59] G. Cavoto,[60] D. del Re,[60] R. Faccini,[14,60] F. Ferrarotto,[60] F. Ferroni,[60]
E. Lamanna,[60] E. Leonardi,[60] M. A. Mazzoni,[60] S. Morganti,[60] G. Piredda,[60] F. Safai Tehrani,[60] M. Serra,[60]
C. Voena,[60] S. Christ,[61] R. Waldi,[61] T. Adye,[62] N. De Groot,[8,62] B. Franek,[62] N. I. Geddes,[62] G. P. Gopal,[62] S. M. Xella,[62]
N. Copty,[63] M. V. Purohit,[63] H. Singh,[63] F. X. Yumiceva,[63] I. Adam,[64] P. L. Anthony,[64] D. Aston,[64] K. Baird,[64]
N. Berger,[64] E. Bloom,[64] A. M. Boyarski,[64] F. Bulos,[64] G. Calderini,[64] M. R. Convery,[64] D. P. Coupal,[64] D. H. Coward,[64]
J. Dorfan,[64] W. Dunwoodie,[64] R. C. Field,[64] T. Glanzman,[64] G. L. Godfrey,[64] S. J. Gowdy,[64] P. Grosso,[64] T. Haas,[64]
T. Himel,[64] T. Hryn'ova,[64] M. E. Huffer,[64] W. R. Innes,[64] C. P. Jessop,[64] M. H. Kelsey,[64] P. Kim,[64] M. L. Kocian,[64]
U. Langenegger,[64] D. W. G. S. Leith,[64] S. Luitz,[64] V. Luth,[64] H. L. Lynch,[64] H. Marsiske,[64] S. Menke,[64] R. Messner,[64]
K. C. Moffeit,[64] R. Mount,[64] D. R. Muller,[64] C. P. O'Grady,[64] V. E. Ozcan,[64] M. Perl,[64] S. Petrak,[64] H. Quinn,[64]
B. N. Ratcliff,[64] S. H. Robertson,[64] L. S. Rochester,[64] A. Roodman,[64] T. Schietinger,[64] R. H. Schindler,[64]
J. Schwiening,[64] V. V. Serbo,[64] A. Snyder,[64] A. Soha,[64] S. M. Spanier,[64] J. Stelzer,[64] D. Su,[64] M. K. Sullivan,[64] H. A. Tanaka,[64]
J. Va'vra,[64] S. R. Wagner,[64] A. J. R. Weinstein,[64] W. J. Wisniewski,[64] D. H. Wright,[64] C. C. Young,[64] P. R. Burchat,[65]
C. H. Cheng,[65] D. Kirkby,[65] T. I. Meyer,[65] C. Roat,[65] R. Henderson,[66] W. Bugg,[67] H. Cohn,[67] A. W. Weidemann,[67]
J. M. Izen,[68] I. Kitayama,[68] X. C. Lou,[68] F. Bianchi,[69] M. Bona,[69] D. Gamba,[69] A. Smol,[69] L. Bosisio,[70]
G. Della Ricca,[70] L. Lanceri,[70] P. Poropat,[70] G. Vuagnin,[70] R. S. Panvini,[71] C. M. Brown,[72] P. D. Jackson,[72] R. Kowalewski,[72]
J. M. Roney,[72] H. R. Band,[73] E. Charles,[73] S. Dasu,[73] F. Di Lodovico,[73] A. M. Eichenbaum,[73] H. Hu,[73] J. R. Johnson,[73]
R. Liu,[73] Y. Pan,[73] R. Prepost,[73] I. J. Scott,[73] S. J. Sekula,[73] J. H. von Wimmersperg-Toeller,[73] S. L. Wu,[73] Z. Yu,[73]
T. M. B. Kordich,[74] and H. Neal[74]

(BABAR Collaboration)

[1]*Laboratoire de Physique des Particules, F-74941 Annecy-le-Vieux, France*
[2]*Università di Bari, Dipartimento di Fisica and INFN, I-70126 Bari, Italy*
[3]*Institute of High Energy Physics, Beijing 100039, China*
[4]*University of Bergen, Institute of Physics, N-5007 Bergen, Norway*
[5]*Lawrence Berkeley National Laboratory and University of California, Berkeley, California 94720*
[6]*University of Birmingham, Birmingham, B15 2TT, United Kingdom*
[7]*Ruhr Universität Bochum, Institut für Experimentalphysik 1, D-44780 Bochum, Germany*
[8]*University of Bristol, Bristol BS8 1TL, United Kingdom*
[9]*University of British Columbia, Vancouver, British Columbia, Canada V6T 1Z1*
[10]*Brunel University, Uxbridge, Middlesex UB8 3PH, United Kingdom*
[11]*Budker Institute of Nuclear Physics, Novosibirsk 630090, Russia*
[12]*University of California at Irvine, Irvine, California 92697*
[13]*University of California at Los Angeles, Los Angeles, California 90024*
[14]*University of California at San Diego, La Jolla, California 92093*
[15]*University of California at Santa Barbara, Santa Barbara, California 93106*
[16]*University of California at Santa Cruz, Institute for Particle Physics, Santa Cruz, California 95064*
[17]*California Institute of Technology, Pasadena, California 91125*
[18]*University of Cincinnati, Cincinnati, Ohio 45221*
[19]*University of Colorado, Boulder, Colorado 80309*
[20]*Colorado State University, Fort Collins, Colorado 80523*
[21]*DAPNIA, Commissariat à l'Energie Atomique/Saclay, F-91191 Gif-sur-Yvette, France*
[22]*Technische Universität Dresden, Institut für Kern-und Teilchenphysik, D-01062 Dresden, Germany*
[23]*Ecole Polytechnique, F-91128 Palaiseau, France*
[24]*University of Edinburgh, Edinburgh EH9 3JZ, United Kingdom*
[25]*Elon University, Elon University, North Carolina 27244-2010*
[26]*Università di Ferrara, Dipartimento di Fisica and INFN, I-44100 Ferrara, Italy*
[27]*Florida A&M University, Tallahassee, Florida 32307*
[28]*Laboratori Nazionali di Frascati dell'INFN, I-00044 Frascati, Italy*
[29]*Università di Genova, Dipartimento di Fisica and INFN, I-16146 Genova, Italy*
[30]*Harvard University, Cambridge, Massachusetts 02138*
[31]*University of Iowa, Iowa City, Iowa 52242*
[32]*Iowa State University, Ames, Iowa 50011-3160*
[33]*Laboratoire de l'Accélérateur Linéaire, F-91898 Orsay, France*
[34]*Lawrence Livermore National Laboratory, Livermore, California 94550*
[35]*University of Liverpool, Liverpool L69 3BX, United Kingdom*
[36]*University of London, Imperial College, London SW7 2BW, United Kingdom*

[37]Queen Mary, University of London, E1 4NS, United Kingdom

[38]University of London, Royal Holloway and Bedford New College, Egham, Surrey TW20 0EX, United Kingdom

[39]University of Louisville, Louisville, Kentucky 40292

[40]University of Manchester, Manchester M13 9PL, United Kingdom

[41]University of Maryland, College Park, Maryland 20742

[42]University of Massachusetts, Amherst, Massachusetts 01003

[43]Massachusetts Institute of Technology, Laboratory for Nuclear Science, Cambridge, Massachusetts 02139

[44]McGill University, Montréal, Québec, Canada H3A 2T8

[45]Università di Milano, Dipartimento di Fisica and INFN, I-20133 Milano, Italy

[46]University of Mississippi, University, Mississippi 38677

[47]Université de Montréal, Laboratoire René J. A. Lévesque, Montréal, Québec, Canada H3C 3J7

[48]Mount Holyoke College, South Hadley, Massachusetts 01075

[49]Università di Napoli Federico II, Dipartimento di Scienze Fisiche and INFN, I-80126 Napoli, Italy

[50]University of Notre Dame, Notre Dame, Indiana 46556

[51]Oak Ridge National Laboratory, Oak Ridge, Tennessee 37831

[52]University of Oregon, Eugene, Oregon 97403

[53]Università di Padova, Dipartimento di Fisica and INFN, I-35131 Padova, Italy

[54]Universités Paris VI et VII, Lab de Physique Nucléaire H. E., F-75252 Paris, France

[55]Università di Pavia, Dipartimento di Elettronica and INFN, I-27100 Pavia, Italy

[56]University of Pennsylvania, Philadelphia, Pennsylvania 19104

[57]Università di Pisa, Scuola Normale Superiore and INFN, I-56010 Pisa, Italy

[58]Prairie View A&M University, Prairie View, Texas 77446

[59]Princeton University, Princeton, New Jersey 08544

[60]Università di Roma La Sapienza, Dipartimento di Fisica and INFN, I-00185 Roma, Italy

[61]Universität Rostock, D-18051 Rostock, Germany

[62]Rutherford Appleton Laboratory, Chilton, Didcot, Oxon OX11 0QX, United Kingdom

[63]University of South Carolina, Columbia, South Carolina 29208

[64]Stanford Linear Accelerator Center, Stanford, California 94309

[65]Stanford University, Stanford, California 94305-4060

[66]TRIUMF, Vancouver, British Columbia, Canada V6T 2A3

[67]University of Tennessee, Knoxville, Tennessee 37996

[68]University of Texas at Dallas, Richardson, Texas 75083

[69]Università di Torino, Dipartimento di Fisica Sperimentale and INFN, I-10125 Torino, Italy

[70]Università di Trieste, Dipartimento di Fisica and INFN, I-34127 Trieste, Italy

[71]Vanderbilt University, Nashville, Tennessee 37235

[72]University of Victoria, Victoria, British Columbia, Canada V8W 3P6

[73]University of Wisconsin, Madison, Wisconsin 53706

[74]Yale University, New Haven, Connecticut 06511

New measurements of D_s^+ and D_s^{*+} meson production rates from B decays and from $q\bar{q}$ continuum events near the $\Upsilon(4S)$ resonance are presented. Using 20.8 fb^{-1} of data on the $\Upsilon(4S)$ resonance and 2.6 fb^{-1} off-resonance, we find the inclusive branching fractions $\mathcal{B}(B \to D_s^+ X) = (10.93 \pm 0.19 \pm 0.58 \pm 2.73)\%$ and $\mathcal{B}(B \to D_s^{*+} X) = (7.9 \pm 0.8 \pm 0.7 \pm 2.0)\%$, where the first error is statistical, the second is systematic, and the third is due to the $D_s^+ \to \phi \pi^+$ branching fraction uncertainty. The production cross sections $\sigma(e^+ e^- \to D_s^+ X) \times \mathcal{B}(D_s^+ \to \phi \pi^+) = 7.55 \pm 0.20 \pm 0.34$ pb and $\sigma(e^+ e^- \to D_s^{*\pm} X) \times \mathcal{B}(D_s^+ \to \phi \pi^+) = 5.8 \pm 0.7 \pm 0.5$ pb are measured at center-of-mass energies about 40 MeV below the $\Upsilon(4S)$ mass. The branching fractions $\Sigma \mathcal{B}(B \to D_s^{(*)+} \bar{D}^{(*)}) = (5.07 \pm 0.14 \pm 0.30 \pm 1.27)\%$ and $\Sigma \mathcal{B}(B \to D_s^{*+} \bar{D}^{(*)}) = (4.1 \pm 0.2 \pm 0.4 \pm 1.0)\%$ are determined from the $D_s^{(*)+}$ momentum spectra. The mass difference $m(D_s^+) - m(D^+) = 98.4 \pm 0.1 \pm 0.3$ MeV/c^2 is also measured.

—————

*Also at Università di Perugia, Perugia, Italy.

†Also at Università della Basilicata, Potenza, Italy.

I. INTRODUCTION

The decay of B mesons into final states involving a $D_s^{(*)+}$ provides an opportunity to study the production mechanisms for $c\bar{s}$ quark pairs.[1] Although several diagrams can lead to $D_s^{(*)+}$ production in B decays, the dominant source [1] is expected to be external $W^+ \rightarrow c\bar{s}$ emission [Fig. 1]. A precise knowledge of this production rate remains interesting in light of continuing theoretical difficulties [2] in accounting for the measurements of both the semileptonic branching fraction and the inclusive charm production rate in B decays. Indeed, it has been noted that an enhanced B decay rate to charm would help explain the small observed semileptonic rate [3].

It is possible to produce $D_s^{(*)+}$ mesons in $q\bar{q}$ events from continuum e^+e^- annihilation. The process of fragmentation (i.e., formation of hadrons) is nonperturbative and can only be modeled phenomenologically. The ratio of vector to pseudoscalar production rates is of particular interest for testing such models. The D_s^+ system is well suited to measure this quantity because the $c\bar{s}$ states with $L=1$ have not been observed to decay to either D_s^+ or D_s^{*+} mesons.

In this Rapid Communication, measurements of $B \rightarrow D_s^+ X$ and $B \rightarrow D_s^{*+} X$ production rates and momentum spectra are presented. We also determine the production cross section for D_s^+ and D_s^{*+} mesons in continuum events.

II. THE BABAR DETECTOR AND DATA SET

The data used for this analysis were collected with the BABAR detector [4] at the PEP-II asymmetric-energy collider [5] at the Stanford Linear Accelerator Center. An integrated luminosity of 20.8 fb^{-1} was recorded in 1999 and 2000 at the $\Upsilon(4S)$ resonance ("on-resonance") corresponding to about 22.7×10^6 produced $B\bar{B}$ pairs, and 2.6 fb^{-1} at an energy of about 40 MeV below the $\Upsilon(4S)$ mass ("off-resonance"). A detailed description of the BABAR detector can be found in Ref. [4]. Only the components of the detector most crucial to this analysis are summarized below.

A five-layer double-sided silicon vertex tracker (SVT) and a 40-layer central drift chamber (DCH) filled with helium-based gas are used to measure the momenta of charged particles. The tracking system covers 92% of the solid angle in the center-of-mass frame and lies within a 1.5-T solenoidal magnetic field. For charged-particle identification, ionization-energy loss (dE/dx) in the DCH and SVT, and Cherenkov radiation detected in a ring-imaging device (DIRC) are used. Photons are identified and measured by a CsI(T1) electromagnetic calorimeter.

---

[1] Reference in this paper to a specific decay channel or state also implies the charge-conjugate decay or state. The notation $D_s^{(*)+}$ means either D_s^+ or D_s^{*+}. $B \rightarrow D_s^{(*)+} \bar{D}^{(*)}$ is a general representation for any of the modes with $c\bar{s}$ and $\bar{c}q$ states including their excited states. The notation $B \rightarrow D_s^{(*)+} X$ also implies $\bar{B} \rightarrow D_s^{(*)+} X$.
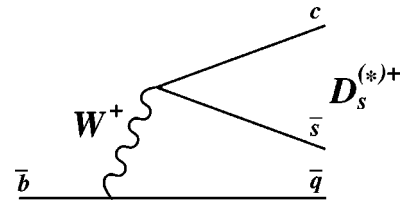

FIG. 1. The main spectator diagram leading to the production of $D_s^{(*)+}$ mesons in B decays.

III. THE D_s^+ AND D_s^{*+} SELECTION

Only the decay mode $D_s^+ \rightarrow \phi\pi^+$ with $\phi \rightarrow K^+ K^-$ is used since it has the best signal-to-background ratio. Charged tracks are required to originate within ± 10 cm of the interaction point along the beam direction and ± 1.5 cm in the transverse plane, and to leave at least 12 hits in the DCH.

Positive kaon identification is required for the tracks forming the candidate ϕ meson. This is based on dE/dx information from the DCH and SVT, and the Cherenkov angle and the number of photons measured with the DIRC. The kaon selection is based on the likelihood calculated for each detector component and uses, for each track, the ratio of likelihoods for the pion and the kaon mass hypotheses, L_π/L_K. If this ratio is less than unity for at least one of the detector subsystems, the particle is selected as a "loose" kaon candidate. A "tight" identification criterion is also used in the analysis, based on the product of the likelihoods for each detector component. In this case, the track is considered a kaon if the ratio of these product likelihoods for the pion- and kaon-mass hypotheses is less than unity.

Three charged tracks originating from a common vertex are combined to form a D_s^+ candidate. Two oppositely charged tracks must be identified as kaons with the "loose" criterion, and at least one of them must pass the "tight" criterion. No identification criteria are applied to the pion from D_s^+ decay. The reconstructed invariant mass of the $K^+ K^-$ candidates must be within 8 MeV/c^2 of the nominal ϕ mass [6]. In the decay $D_s^+ \rightarrow \phi\pi^+$, the ϕ meson is polarized longitudinally and therefore the angular distribution of the kaons has a $\cos^2\theta_H$ dependence, where θ_H is the angle between the K^+ and D_s^+ in the ϕ rest frame. We require $|\cos\theta_H| > 0.3$, which Monte Carlo studies show retains 97% of the signal while rejecting about 30% of the background.

With these requirements, signals for $D_s^+ \rightarrow \phi\pi^+$ and the Cabibbo-suppressed decay $D^+ \rightarrow \phi\pi^+$ are readily observed [Fig. 2(a)]. The D_s^+ and D^+ peaks are both fit with single Gaussian distributions with a common free width. We model the combinatorial background with an exponential function. From the fit a D_s^+ signal of $47\,794 \pm 311$ events is found with a mass difference $m(D_s^+) - m(D^+)$ of $98.4 \pm 0.1 \pm 0.3$ MeV/c^2. The first error on the latter is statistical, and the second is systematic, obtained from a study of the mass difference as a function of momentum in both data and Monte Carlo simulation. Although the uncertainties in the absolute mass scale are on the order of several MeV/c^2, the systematic error in the determination of the D_s^+ and D^+ mass difference is much smaller, since many sources of error cancel.
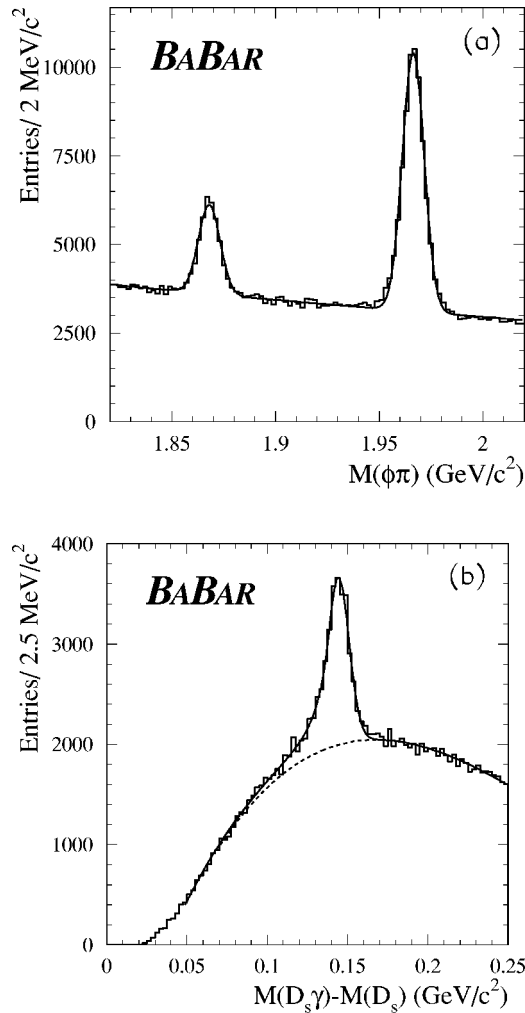
FIG. 2. (a) The $\phi\pi$-invariant mass spectrum. In addition to the D_s^+ signal, candidates for the Cabibbo-suppressed decay $D^+ \to \phi\pi^+$ are also observed. The fit function is a single Gaussian for each peak, with widths constrained to be equal, plus an exponential background. (b) Distribution of the mass difference $\Delta M = M_{D_s^+ \gamma} - M_{D_s^+}$. The fit function is a Crystal Ball function for the signal plus a threshold function, as described in the text.

Candidate D_s^{*+} mesons are reconstructed in the decay $D_s^{*+} \to D_s^+ \gamma$, with the subsequent decay $D_s^+ \to \phi\pi^+$. D_s^+ candidates are selected by requiring the $\phi\pi$-invariant mass to be within 2.5 standard deviations (σ) of the fitted peak value. These D_s^+ candidates are then combined with photon candidates in the event. Photon candidates are required to satisfy $E_\gamma > 50$ MeV, where E_γ is the photon energy in the laboratory frame, and $E_\gamma^* > 110$ MeV, where E_γ^* is the photon energy in the $\Upsilon(4S)$ center of mass. When combined with any other photon in the event, the photon candidate should not form a π^0, defined by a total center-of-mass energy $E_{\gamma\gamma}^* > 200$ MeV and an invariant mass $115 < M_{\gamma\gamma} < 155$ MeV/c^2. The distribution of the mass difference $\Delta M = M(D_s^+ \gamma) - M(D_s^+)$ is shown in Fig. 2(b).

The ΔM distribution of the signal is parametrized with an asymmetric function to account for energy leakage and calorimeter shower shape fluctuations. The signal is modeled

with a Crystal Ball function [7], which incorporates a Gaussian core with a power-law tail toward lower masses. For the background, a threshold function

$$f(\Delta M) = p_1(\Delta M - p_2)^{p_3} e^{p_4(\Delta M - p_2)}$$

is used, where the four parameters p_i are free in the fit. After ensuring that the connection point between the Gaussian and power-law tail does not depend on momentum and agrees with Monte Carlo simulation, this parameter has been fixed to 0.89σ in the final fit. A signal with $14\,392 \pm 376$ D_s^{*+} events is observed.

IV. EXTRACTION OF $D_s^{(*)+}$ MOMENTUM SPECTRA

The momentum spectrum of D_s^+ mesons in the e^+e^- center-of-mass frame is extracted by fitting the $\phi\pi$-invariant mass distribution for 24 ranges of D_s^+ candidate momentum. These ranges are 200 MeV/c wide, which is much larger than the momentum resolution (≈ 6 MeV/c). The same function with two single Gaussians described above for the fit to the full mass distribution is used as well for the individual momentum bins. Since there are many more events in the on-resonance data sample, the number of D_s^+ in the off-resonance data is extracted with the Gaussian parameters (M_{D^+}, $M_{D_s^+}$, and σ) fixed to the values obtained from the on-resonance data.

The center-of-mass momentum spectrum for D_s^{*+} mesons is extracted by fitting the ΔM-invariant mass distribution in 250 MeV/c-wide D_s^{*+} momentum ranges. We use a larger range because the D_s^{*+} yield is lower. The ΔM distributions are modeled with a Crystal Ball function for the signal and a threshold function for the background as described above for the fit to the full distribution. The off-resonance data are again fit with the Gaussian parameters ($\bar{x}$ and σ) fixed to the values obtained from the on-resonance data.

The efficiency ϵ, obtained from Monte Carlo simulation of $B\bar{B}$ and $c\bar{c}$ events, varies as a function of the $D_s^{(*)+}$ center-of-mass momentum p^*. The efficiency ranges from 20% (5%) when the D_s^+ (D_s^{*+}) is at rest to 40% (20%) for $p^* = 5$ GeV/c. The efficiency-corrected momentum spectra of D_s^+ and D_s^{*+} are shown in Fig. 3.

V. INCLUSIVE BRANCHING FRACTIONS

The D_s^+ and D_s^{*+} production cross sections in $q\bar{q}$ continuum are obtained by integrating the momentum spectra obtained from the off-resonance data. This gives

$$\sigma(e^+e^- \to D_s^\pm X) \times \mathcal{B}(D_s^+ \to \phi\pi^+) = 7.55 \pm 0.20 \pm 0.34 \text{ pb},$$

$$\sigma(e^+e^- \to D_s^{*\pm} X) \times \mathcal{B}(D_s^+ \to \phi\pi^+) = 5.8 \pm 0.7 \pm 0.5 \text{ pb},$$

where the first error is statistical and the second systematic. Sources of systematic error are listed in Table I. These include the statistical precision of the Monte Carlo determination of the efficiency, the luminosity uncertainty, and contributions from residual uncertainties on tracking (1.2% per track), and particle identification efficiencies, which are de-
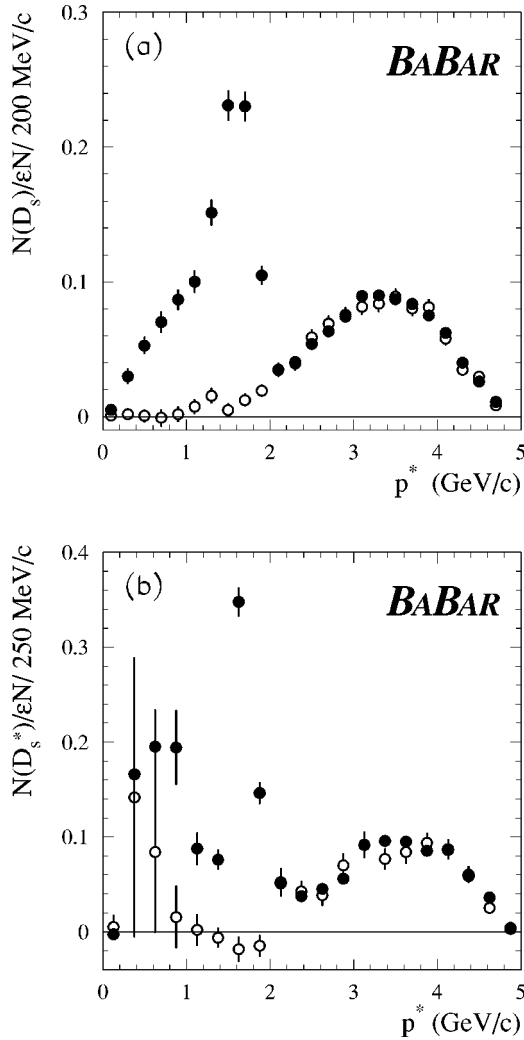
FIG. 3. Efficiency-corrected center-of-mass momentum spectra for (a) D_s^+ and (b) D_s^{*+} for on-resonance (filled circles) and scaled off-resonance data (open circles).

termined from control samples in data. In addition, for the $D_s^{*\pm}X$ measurement, there are contributions from the uncertain signal shape, and residual uncertainties on the photon and π^0 veto efficiencies, again determined with control samples.

In order to determine the momentum spectra for $D_s^{(*)+}$ mesons from B meson decays, the off-resonance data are scaled by the on- to off-resonance luminosity ratio and then subtracted bin by bin from the on-resonance data. Integrating the resulting spectrum after continuum subtraction and efficiency correction gives a total D_s^+ yield from B meson decays of $87\,711 \pm 1485$ events. This corresponds to an inclusive branching fraction of

$$\mathcal{B}(B \to D_s^+ X) = \left[(10.93 \pm 0.19 \pm 0.58) \frac{(3.6 \pm 0.9)\%}{\mathcal{B}(D_s^+ \to \phi \pi^+)} \right]\% .$$

Likewise, the total D_s^{*+} yield from B meson decays is $60\,047 \pm 6201$ events, leading to the inclusive branching fraction of

TABLE I. Systematic errors for cross-section and branching fraction measurements.

| | Fractional error (%) | | | |
| | Continuum | | B decays | |
Source	$D_s^+ X$	$D_s^{*+} X$	$D_s^+ X$	$D_s^{*+} X$
Signal shape		3.0	0.5	3.0
Background subtraction			0.4	4.2
Monte Carlo statistics	1.0	4.8	2.5	4.2
Bin width			1.4	2.0
Total for $D_s^{(*)+}$ yield	1.0	5.7	2.9	7.0
Luminosity/$N(B\bar{B})$	1.5	1.5	1.6	1.6
$\mathcal{B}(\phi \to K^+ K^-)$	1.6	1.6	1.6	1.6
Particle identification	1.0	1.0	1.0	1.0
Tracking efficiency	3.6	3.6	3.6	3.6
$\mathcal{B}(D_s^{*+} \to D_s^+ \gamma)$		2.7		2.7
Photon efficiency		1.3		1.3
π^0		2.7		2.7
Total systematic error	4.5	8.2	5.3	9.0

$$\mathcal{B}(B \to D_s^{*+} X) = \left[(7.9 \pm 0.8 \pm 0.7) \frac{(3.6 \pm 0.9)\%}{\mathcal{B}(D_s^+ \to \phi \pi^+)} \right]\% .$$

In the results above, the first error is statistical and the second is systematic. The dominant error, due to the uncertainty in the $D_s^+ \to \phi \pi^+$ branching fraction of $(3.6 \pm 0.9)\%$ [6], is shown separately. It is important to note that, with this method, the result is independent of any assumption regarding the shape of the fragmentation function. The various contributions to the systematic error are listed in Table I. In addition to the sources already noted above, the uncertainty in the shape of the background impacts this measurement, particularly in the lower momentum bins. This contribution is estimated with the use of different parametrizations for the background shape and different methods for handling the continuum subtraction. The efficiency variation over the width of the momentum bins is also included as an additional systematic error.

VI. FITS TO $D_s^{(*)+}$ MOMENTUM SPECTRA

By fitting the $D_s^{(*)+}$ momentum spectrum, relative branching fractions of B decays to different final states containing $D_s^{(*)+}$ mesons are obtained. In the $\Upsilon(4S)$ rest frame, two-body B decays produce $D_s^{(*)+}$ mesons with a momentum spectrum about 300 MeV/c wide. In B decays, the $D_s^{(*)+}$ momentum spectrum is essentially governed by the production of direct $D_s^{(*)+}$. Other $c\bar{s}$ states (with $L=1$), such as $D_{s1}^+(2536)$ and $D_{s2}^{*+}(2573)$, primarily decay to $D^{(*)}K$. Because D_s^{*+} decays to $D_s^+ \gamma$ or $D_s^+ \pi^0$, the D_s^+ momentum distribution is slightly broader and shifted downward compared to direct production from $B \to D_s^+ X$.

Three different sources of $D_s^{(*)+}$ mesons in B decays are considered for the fits to the momentum spectra.

(1) $B \to D_s^{(*)+} \bar{D}^{(*)}$ decays. The relative branching frac-

tions of the individual channels can be taken either from existing measurements [8] or from predictions that assume factorization [9–11]. The fit is performed for both cases, with the assumption $f_{D_s^{(*)+}} = f_{D_s^+}$ for the theoretical models, where $f_{D_s^{(*)+}}$ are the $D_s^{(*)+}$ decay constants.

(2) $B \rightarrow D_s^{(*)+} \bar{D}^{**}$ decays. Four $\bar{D}^{**}$ states are considered: $\bar{D}_0^*(j=\frac{1}{2})$, $\bar{D}_1(2420)$, $\bar{D}_1(j=\frac{1}{2})$, and $\bar{D}_2^*(2460)$. Observation of $B \rightarrow D_s^{(*)+} \bar{D}^{**}$ decays was recently reported by CLEO [12].

(3) Three-body $B \rightarrow D_s^{(*)+} \bar{D}^{(*)} \pi/\rho/\omega$ decays. Since little is known about these decays, they are attributed equal weights, and the momentum distributions are generated according to phase space.

Minimum-χ^2 fits to the $D_s^{(*)+}$ momentum spectra are performed, where the total number of $D_s^{(*)+}$ events and the fractions of the source (1) and (2) contributions are free parameters. From the fits to the D_s^+ and D_s^{*+} spectra, the ratios of two-body modes [source (1)] to the total inclusive rate are determined to be

$$\frac{\Sigma \mathcal{B}(B \rightarrow D_s^{(*)+} \bar{D}^{(*)})}{\mathcal{B}(B \rightarrow D_s^+ X)} = (46.4 \pm 1.3 \pm 1.4 \pm 0.6)\%,$$

$$\frac{\Sigma \mathcal{B}(B \rightarrow D_s^{*+} \bar{D}^{(*)})}{\mathcal{B}(B \rightarrow D_s^{*+} X)} = (53.3 \pm 3.7 \pm 3.1 \pm 2.1)\%.$$

The first error is statistical. The second error represents the systematic error due to the limited Monte Carlo statistics and the background parametrization.

The last error is due to the model uncertainty. It is obtained by varying the relative fractions of the modes contributing to each source of $D_s^{(*)+}$ listed above. The fit is performed with alternative assumptions for the relative contributions of the modes in source (1) taken from theoretical predictions and measurements. Different weights for $B \rightarrow D_s^+ \bar{D}^{**}$ and $B \rightarrow D_s^{*+} \bar{D}^{**}$, as well as different relative branching fractions of the four modes within source (2), are used. For source (3), either $B \rightarrow D_s^{(*)} \bar{D}^{(*)} \pi$, or $B \rightarrow D_s^{(*)} \bar{D}^{(*)} \rho/\omega$ is assumed to be dominant. The χ^2 of the fit for the inclusive D_s^{*+} momentum spectrum is lowest when the contribution of $B \rightarrow D_s^* \bar{D}^{(*)} \rho/\omega$ is dominant compared to $B \rightarrow D_s^* \bar{D}^{(*)} \pi$. Uncertainty in source (3) is the main contribution to the error due to model dependence. The results of the fits to the $D_s^{(*)+}$ momentum spectra are shown in Fig. 4 under the assumption of equal weights for the individual contributions within sources (2) and (3), and with the weights of the individual modes of source (1) taken from [11].

The sum of branching fractions for the two-body $B \rightarrow D_s^{(*)} \bar{D}^{(*)}$ decays are obtained from the fits to the $D_s^{(*)+}$ momentum spectra, where the yield from each source is a free parameter. We find
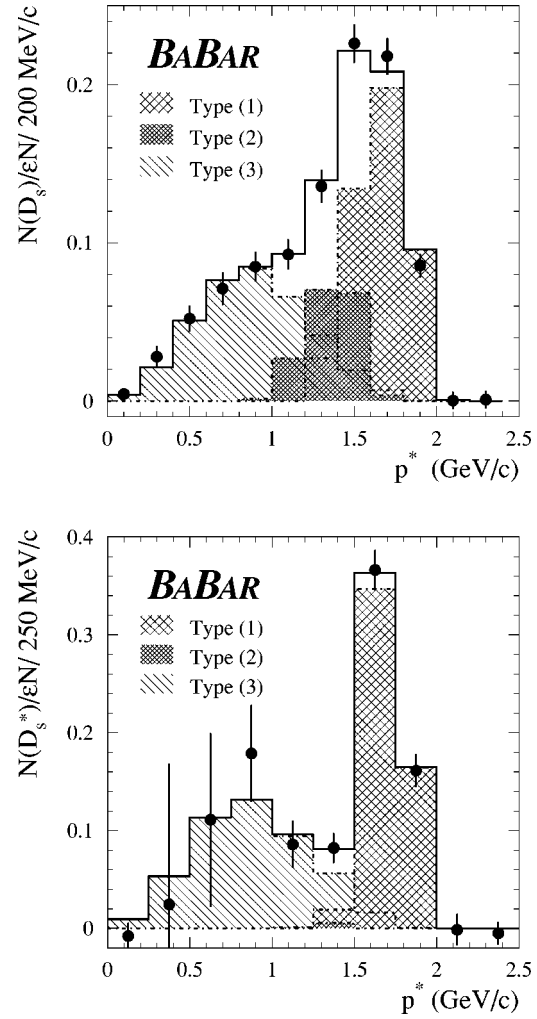

FIG. 4. Fit results for D_s^+ (top figure) and D_s^{*+} (bottom figure) momentum spectra. The data are dots with error bars, and the histograms are the components of the fit function described in the text. Type (1) is $B \rightarrow D_s^{(*)+} \bar{D}^{(*)}$, type (2) is $B \rightarrow D_s^{(*)+} \bar{D}^{**}$, and type (3) is $B \rightarrow D_s^{(*)+} \bar{D}^{(*)} \pi/\rho/\omega$. The solid histogram is the sum of the three components.

$$\Sigma \mathcal{B}(B \rightarrow D_s^{(*)+} \bar{D}^{(*)}) = (5.07 \pm 0.14 \pm 0.30 \pm 1.27)\%,$$

$$\Sigma \mathcal{B}(B \rightarrow D_s^{*+} \bar{D}^{(*)}) = (4.1 \pm 0.2 \pm 0.4 \pm 1.0)\%,$$

where the first error is statistical, the second is systematic, and the third is due to the $D_s^+ \rightarrow \phi \pi^+$ branching fraction uncertainty. The systematic error includes contributions from the $B \rightarrow D_s^{(*)+} X$ branching fractions, the relative contributions of source (1), and the model dependence of the source spectra. The sum of the two-body modes is reasonably separated in the momentum spectra from the other components. Therefore, the fractional error on the sum of the two-body

modes is smaller than the fractional error on the $B \rightarrow D_s^{(*)+}X$ branching fraction or the relative two-body branching ratio.

VII. SUMMARY

In summary, the branching fractions for inclusive $B \rightarrow D_s^{(*)+}X$ production have been determined as well as the $D_s^{(*)+}$ production cross-sections from continuum events at center-of-mass energies about 40 MeV below the $\Upsilon(4S)$ mass. Our more precise results for the D_s^+ are in agreement with previous measurements [8,13], while the D_s^{*+} measurements are new. In contrast to previous results, our measurements do not rely on any assumptions regarding the shape of the fragmentation function. Finally, fits to the $D_s^{(*)+}$ momentum spectra provide relative yields and branching fractions

for two-body $B \rightarrow D_s^{(*)+}\bar{D}^{(*)}$ and $B \rightarrow D_s^{*+}\bar{D}^{(*)}$ decays. The mass difference $m(D_s^+) - m(D^+)$ has also been measured.

[1] V. Jain, Nucl. Phys. B (Proc. Suppl.) **50**, 96 (1996); CELO Collaboration, T. E. Coan *et al.*, Phys. Rev. Lett. **80**, 1150 (1998).

[2] I. Bigi *et al.*, Phys. Lett. B **323**, 408 (1994).

[3] A. F. Falk, M. B. Wise, and I. Dunietz, Phys. Rev. D **51**, 1183 (1995).

[4] BABAR Collaboration, B. Aubert *et al.*, Nucl. Instrum. Methods Phys. Res. A **479**, 1 (2002).

[5] PEP-II Conceptual Design Report, SLAC-R-418 (1993).

[6] Particle Data Group, D. E. Groom *et al.*, Eur. Phys. J. C **15**, 1 (2000).

[7] The ΔM distribution for the $D_s^+ \gamma$ signal is fit with the Crystal Ball function

$$f(x) = N \times \begin{cases} \exp\left(-\dfrac{(x-\bar{x})^2}{2\sigma^2}\right), & (\bar{x}-x)/\sigma > \alpha \\ A \times \left(B - \dfrac{x-\bar{x}}{\sigma}\right)^{-n}, & (\bar{x}-x)/\sigma \leq \alpha, \end{cases}$$

where $A \equiv (n/|\alpha|)^n \times \exp(-|\alpha|^2/2)$ and $B \equiv (n/|\alpha|) - |\alpha|$. N is a normalization factor, $\bar{x}$ and σ are the peak position and width of the Gaussian portion of the function, α is the point at which the function changes to the power function, and n is the exponent of the power function. A and B are defined so that the function and its first derivative are continuous at α. More details can be found in D. Antreasyan, Crystal Ball Note 321 (1983).

[8] CLEO Collaboration, D. Gibaut *et al.*, Phys. Rev. D **53**, 4734 (1996).

[9] M. Bauer *et al.*, Z. Phys. C **34**, 103 (1987).

[10] J. Rosner, Phys. Rev. D **42**, 3732 (1990).

[11] M. Neubert and V. Rieckert, Nucl. Phys. **B382**, 97 (1992).

[12] CELO Collaboration, S. Ahmed *et al.*, Phys. Rev. D **62**, 112003 (2000).

[13] ARGUS Collaboration, H. Albrecht *et al.*, Z. Phys. C **54**, 1 (1992).